3D RECONSTRUCTION WITH AN AUV MOUNTED FORWARD-LOOKING SONAR

Douglas Horner Naval Postgraduate School
Nevin McChesney Naval Postgraduate School
Tad Masek Naval Postgraduate School
Sean Kragelund Naval Postgraduate School

Naval Postgraduate School
Center for Autonomous Vehicle Research
Mechanical and Aeronautical Engineering
Monterey, CA 93943-5000
dphorner@nps.edu
tdmasek@nps.edu
spkragel@nps.edu

*Abstract*: **The paper discusses the use of dual stave forward-looking sonar to build a three-dimensional underwater model for navigation in restricted waterways. The sonar normally provides separate horizontal and vertical images but when the information is synthesized into a single three-dimensional model it permits, in certain circumstances, the AUV to plan and carry out a trajectory where no path is otherwise available. As the sonar system is fixed mounted to the AUV body, a trajectory is presented which uses the combined sonar fields-of-view to produce paths that optimize situational understanding for reactive and deliberative obstacle avoidance.**

1.0 INTRODUCTION

Currently Autonomous Underwater Vehicles (AUV) are used primarily in open oceans where the primary danger to the vehicles are from unexpected navigation hazards on the ocean floor and surface. More and more, vehicles are being tasked with collecting information in more congested, restrictive waterways such as harbors and rivers. Due to the dynamism of the environment, it requires an AUV to have more flexibility in path planning and reactive avoidance behaviors. This requirement for greater perceptual awareness is made possible through deliberate navigation strategies for map building.

Forward Looking Sonar has developed to the point that small AUVs can use it for obstacle detection, avoidance [1,2] and map building. The configuration of the sonar produces separate horizontal and vertical images.

Two examples of sonar images are given in Figures one and two. These images were taken as the AUV approached a bridge. Notice that in the horizontal image there is a strong intensity across the entire field of view at approximately 30 meters distance from the vehicle. This is the underwater ground buildup to support the bridge pylons. At about 45 meters from the vehicle are the bridge pylons, these appear as vertical lines in the image.
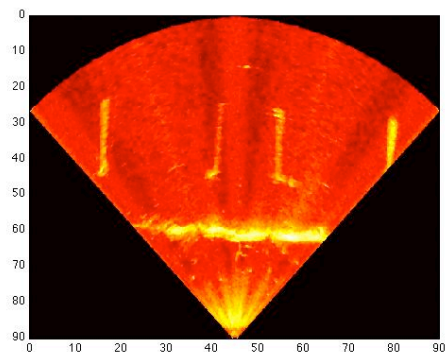
Figure 1. Horizontal Sonar Image – AUV approaches bridge

Figure two is a vertical sonar image taken at approximately the same time. It includes annotations for the riverbed, river surface and pylon(s) obstructing the vehicle's path forward. In other words, automated image processing and path planning algorithms wouldn't be able to produce a trajectory underneath the bridge using either of the images. It will be shown that only by combining horizontal and vertical sonar models together with the intensity images over time, is it possible to develop a viable, safe path underneath the bridge.
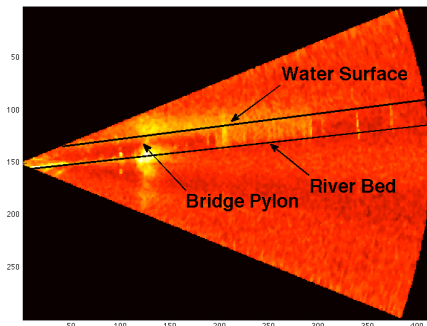
Figure 2. Vertical Sonar Image – AUV approaches bridge

Since the sonar system is fixed to the nose of the AUV body, the only way to slew the horizontal and vertical sonar staves is through the vehicle actuation. Non-linear trajectories can be designed to maximize the situational understanding for the AUV. This is necessary to more fully understand the environment forward of the AUV for making time-critical decisions associated with collision-free paths. These trajectories must be developed in real-time and take into consideration the vehicle dynamics, sensory information and situational understanding represented by its internal map.

The paper discusses the following: First it describes the AUV and sonar used in the developmental testing. Second, it develops a three-dimensional model of the horizontal and vertical sonar staves. Third, it discusses the use of probabilistic occupancy grids to build an internal representation of the environment. Fourth, it discusses the image processing techniques necessary to deal with noise sources that inhibit accurate map building. Fifth, it discusses results based on data sets collected in the Charles River, Cambridge MA with an AUV

navigating in and around the Massachusetts Avenue Harvard Bridge. Sixth, it discusses a control law for maximizing situational awareness in restricted waterway areas.

2.0 SYSTEM DESCRIPTION

The system used for the research is a modified REMUS 100 AUV with the Blueview Forward Looking Sonar and is listed in Figure 3. The sonar module contains a secondary or "backseat" CPU controller that permits real-time sonar image processing and path planning. The AUV has a communication protocol that permits the backseat controller to take overriding control; this functionality is very useful for prototyping autonomous behaviors.

Figure 3. NPS REMUS AUV

2.1 AUV DESCRIPTION

The Charles River data set was collected on a REMUS specially configured with an Integrated Navigation System (INS) that provided accurate position estimation to within .5 percent distance traveled by combining together accurate accelerometers and rate gyros with velocity estimates from the Doppler Velocity Log (DVL) and position fixes from a GPS[1]. The starting point for the missions was the MIT Sailing Pavilion dock.

2.2 SONAR DESCRIPTION

The Blueview P450-15E Forward Looking Sonar was mounted to the front of the AUV. The sonar

has four horizontally mounted staves that produce a single image with a ninety degree field of view. The sonar also has two vertically mounted staves that produce a forty-six degree field of view and result in a single, vertical image. In each case the range resolution is approximately 2 inches and the bearing resolution is approximately 1 degree.

3.0 SONAR MODELING

The image created by the sonar is a two-dimensional representation of a three-dimensional volume. A depiction of a nominal volume ensonified by the horizontally sonar is depicted in Figure 5.
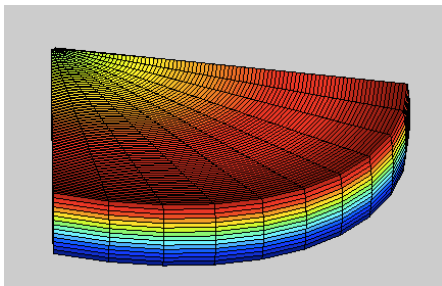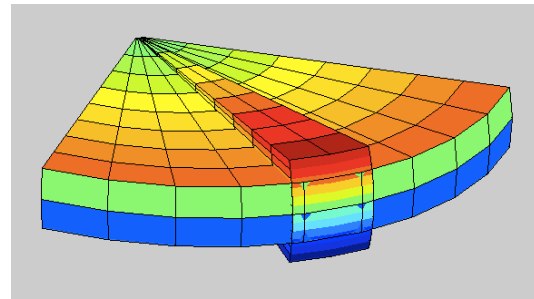

Figure 5. Horizontal Sonar Model

A single stave of the P450-15E has an approximate 23-degree field of view in the image plane. The ensonified volume covers a fifteen-degree spread in the vertical plane. The sonar is unable to distinguish differences of an object at different elevations within this region. For example, the object highlighted in Figure 6, could be located anywhere within the fifteen-degree spread. Based on the corresponding distance from the AUV this is a spread of +- 4 meters. This is the ambiguity of the sonar in the vertical plane.
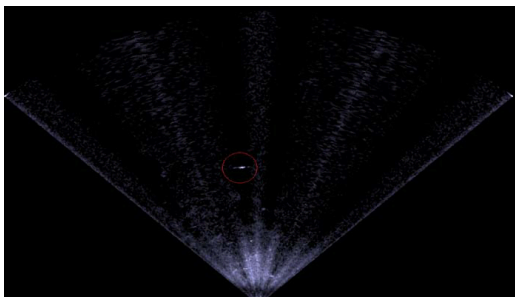
Figure 6. Horizontal Image with circled object 30 meters from the AUV.

The vertical array is composed of a two staves mounted perpendicular to the horizontal array. Mounting the array in this fashion provides angular resolution in the vertical direction. Due to the rotation of the array, the ambiguity of the sonar shifts to the horizontal direction. All vertical sonar images will have fifteen degrees of ambiguity in the horizontal direction. The vertical sonar is used to provide the location of the ocean floor and the height of the objects encountered proud of the ocean floor. The vertical sonar head is rigidly mounted on the AUV with an approximate 5 degree downward angle.

By combining the separate fields of view, the two sonars can effectively create a volume with resolution in all three planes. The volume ensonified by the combination of sonars is depicted in Figure 7.

Figure 7. A combined sonar model depicting the vertical and horizontal forward looking sonar

Of particular relevance is the fifteen by fifteen-degree area where the two arrays overlap. By combining the resolution of each sonar, it effectively creates a cross section where the resolution is two inches in range and one degree in vertical width and one degree in horizontal width.

3.1 GEO-LOCATING IMAGE DATA

The sonar system is fixed mounted to the front of the vehicle. The FLS data is referenced to the vehicle's position; it has a local reference frame. To be useful, the data needs to be transformed into the global space. By combining together the vehicle position with the FLS model each data point can be geo-located. This results in the following equations for translating a locally referenced sonar image pixel into a global reference frame.

$$x_p = x_v + r_p \cos(\theta_v + \theta_p)\cos(\phi_v + \phi_p)$$
$$y_p = y_v + r_p \sin(\theta_v + \theta_p)\cos(\phi_v + \phi_p)$$
$$z_p = z_v + r_p \sin(\phi_v + \phi_p)$$

Where (x_p, y_p, z_p) is the globally referenced location of the pixel The above equations will map data stored in the image space into the global space.

The next step is to separate detections from image noise. This will be done through the use of occupancy grids where the elements in each grid will be converted from an intensity pixel to a probability of an object being located in the grid cell.

4.0 OCCUPANCY GRIDS

To permit deliberative and reactive path planning a robot needs an internal representation of it's external environment – in other words it needs a map. To create a safe path the vehicle needs to know the location of obstacles and the location of free space. An additional requirement for the vehicle is to create obstacle-free trajectories that are globally consistent and not subject to trapping conditions - normally described as local minima. Probabilistic occupancy grids are an appropriate and accepted methodology for building and maintaining an internal map [4]. In this case the goal is to build and maintain a three-dimensional occupancy grid that is used for real-time path planning.

Occupancy grids divide the environment into gridded cells. Each cell is evaluated to determine whether or not an object is present. The range of values of each cell is between 0 (no object present) and 1 (object present). The cells are initialized to .5, which represents impartiality of an obstacle presence. Because it is not necessary to recognize and organize objects in the underwater map by their shape and location, occupancy grids is an appropriate methodology for avoidance maneuvers.

Bayes Theorem is used to determine the probability of the state of the cell given the current reading from the sonar. Based on this, Elfes provides an iterative solution to determining the probability that a cell is occupied given all previous measurements.

$$P\left[s(C) = OCC \mid \{r\}_{t+1}\right] =$$
$$\frac{P\left[r_{t+1} \mid s(C) = OCC\right] * P\left[s(C) = Occ \mid \{r\}_t\right]}{\sum_{\forall s(C)} P\left[r_{t+1} \mid s(C)\right] * P\left[s(C) \mid \{r\}_t\right]}$$

r_{t+1} : The current measurement

$s(C)$: State of the cell

$\{r\}$: All measurement up to time t

The definitions of the terms are as follows:

$P\left[s(C) = Occ \mid \{r\}_{t+1}\right]$	Prob a cell is occupied given the current and all prior measurements
$P\left[s(C) = Occ \mid \{r\}_t\right]$	Prob a cell is occupied given all the prior measurements
$P\left[s(C) = Empty \mid \{r\}_t\right]$	Prob a cell is empty given all the prior measurements
$P\left[r_{t+1} \mid s(C) = Occ\right]$	Prob of receiving the current measurement given the cell is occupied
$P\left[r_{t+1} \mid s(C) = Empty\right]$	Prob of receiving the current measurement given the cell is empty

Table 1. Definition of terms

The summation in the denominator represents two cases – either the cell is occupied or empty. Since the cells can have only two states $P\left[s(C) = Empty \mid \{r\}_t\right]$ can be replaced by $1 - P\left[s(C) = Occ \mid \{r\}_t\right]$. As an example, assume that an occupancy grid cell has a prior probability $P\left[s(C) = Occ \mid \{r\}_t\right] = .6$, and a new measurement arrives. Based on the new measurement and the corresponding probability distributions the values of $P\left[r_{t+1} \mid s(C) = Occ\right]$ and $P\left[r_{t+1} \mid s(C) = Empty\right]$ are determined. Assume those are respectively equal to .2 and .4. From these values the probability of the cell being occupied is updated.

$$P\left[s(C) = Occ \mid \{r\}_{t+1}\right] =$$
$$\frac{0.4 * 0.6}{0.2 * (1 - .6) + 0.4 * 0.6} = .75$$

As the AUV navigates, an update occurs for each globally mapped occupancy grid cell. In other words, as the sonar sensor information becomes available the range of updated cells reflects the transformed local sensor information into the global map. The next step is to determine the two probability distributions given the cell is either empty or occupied.

4.1 FORWARD LOOKING SONAR PROBABILITY MODELS

To populate an occupancy grid, requires the development of probability models for the FLS. For a sensor to be used in an occupancy grid, two separate probabilistic models need to be generated. One model describes the probability of receiving a value when the return can be attributed solely to noise. The second model describes the probability of receiving a particular value when the sonar return can be attributed to a physical object.

The development of the models is made more difficult from the sporadic noise generated by the forward-looking sonar. Noise is generated by both internal and external sources. The noise sources internal to the vehicle include power supply fluctuations, Acoustic Doppler Current Profiler (ADCP) and the Acoustic Modem. Noise sources external to the vehicle includes weather, biological sources and other vehicles or man-made sources. To begin we will discuss the background FLS noise model. This methodology is applicable for both the horizontal and vertical images.

4.1.1 BACKGROUND NOISE MODEL

The blazed array sonar system utilizes a principle similar to echelette diffraction gratings in optics to create a multitude of beams from a single sound source [6]. The blazed sonar array maps the frequency of a given broadband pulse to the angular spatial domain. This creates an image that contains a low intensity random signal that varies with bearing angle. Because it varies, a uniform threshold filter is insufficient for describing the background noise.

To adequately handle this image diversity, it is necessary to develop a per pixel noise model. To do so we took a data set of 300 sonar images that contained few objects in the field of view. Because of the multitude of noise sources a histogram was used to observe the distribution.
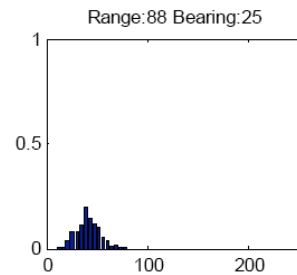
The histogram contained 25 bins with an approximate spacing of the image intensity values of 160. Figures 9a, 9b and 9c give examples of histogram distributions.
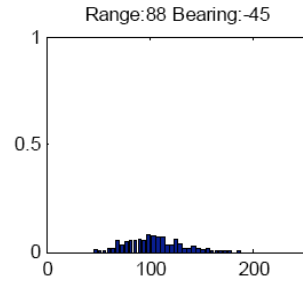
Figure 9a. Noise Histogram for the horizontal FLS at Range 88m and -45 degrees bearing
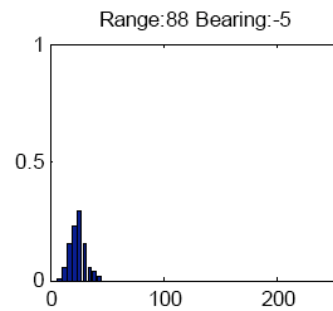
**Figure 9b**. Noise Histogram for the horizontal FLS at Range 88m and -5 degrees bearing

Figure 9c. Noise Histogram for the horizontal FLS at Range 88m and 25 degrees bearing

4.1.2 OBJECT DETECTION MODEL

The process to develop the object detection model was similar to the background noise model. Since the object detections were not as common on a per pixel basis and the intensity from an object in the sonar return was not as prone to intensity fluctuations over bearing and range, a single global model was developed. To create the model 200 images in each plane were annotated using the LabelMe annotation tool. Then the areas containing only objects were

extracted and a 25 bin histogram was created of the intensities for each plane. Figure 10 gives a plot of the pixel intensities from the objects selected from the horizontal images. This normalized histogram can be then used as the detection probability distribution.
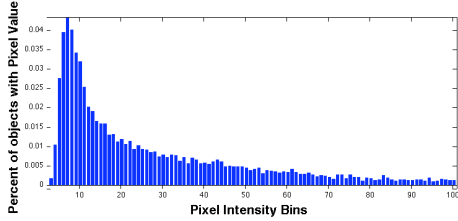
Figure 10. Normalized histogram of pixel intensities from selected objects in horizontal sonar images. Note the graphic has been truncated in the x axis for viewing.

4.1.3 COMBINING MULTIPLE SENSORS

Our goal is to create a single sonar model from both the horizontal and vertical systems. Our methodology is to maintain separate occupancy grids and combine them using an independent opinion pool. Assuming the sonar creates occupancy grids P_1 and P_2. The grid probabilities can be combined as a pooled probability:

$$\frac{P_1 P_2}{P_1 P_2 + (1 - P_1)(1 - P_2)}$$

The individual occupancy grid values are dependent only on the sensor input and its probabilistic model. Maintaining the independence between sensors permits greater flexible in adding or subtracting sensors. For example, if the AUV also had a side-looking sonar, it could be used as another sensor in the future for enhancing accuracy of the occupancy grid. Compared with other approaches this is also computationally less intensive and more appropriate for real-time robotic applications.

5. RESULTS

The AUV was deployed on the Charles River and sent on a path underneath the Massachusetts Avenue Harvard Bridge. Figure 11 shows an overhead trajectory plot with the bridge pylon positions. GPS positions of the pylons were acquired by placing a handheld GPS in close proximity to the pylons under the bridge. The multiple position plots reflect the inconsistency of the GPS readings due to the bridge occluding satellite reception.

Figures 1 and 2 showed examples of the vertical and horizontal images as the AUV approached the bridge. Because of the obstacles seen in the images the AUV would not be able to navigate successfully between the pylons and over the berm if it relied on processing each image separately.
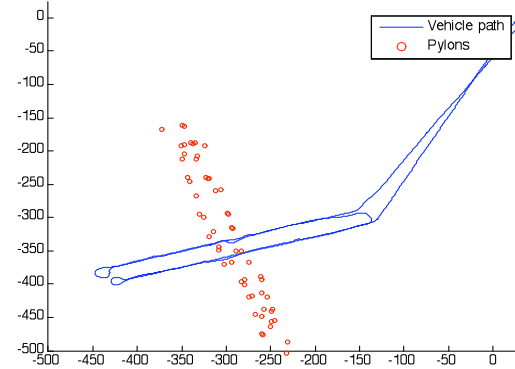
Figure 11. AUV trajectory with annotated positions of bridge pylons

Figure 12 shows the horizontal occupancy grid with the bridge pylon GPS positions plotted. Gridded cells in black indicate a probability of .98 or greater that an object exists. It can be seen that by itself there is not a clear path under the bridge.
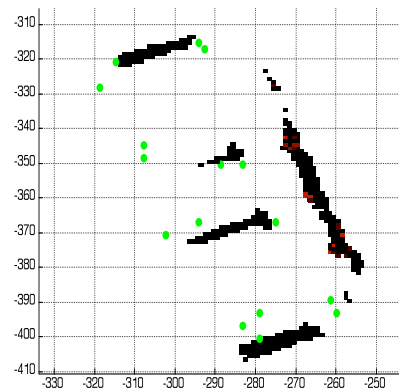
Figure 12. Horizontal occupancy grid with GPS fixes of bridge pylons (in green)

Figure 13 shows the three-dimensional map. By combining together both the vertical and horizontal occupancy grids into a single

representation, a viable path is now available to the vehicle to pass underneath the bridge. Only through the combination of horizontal and vertical FLS and three-dimensional occupancy grid does the path emerge.
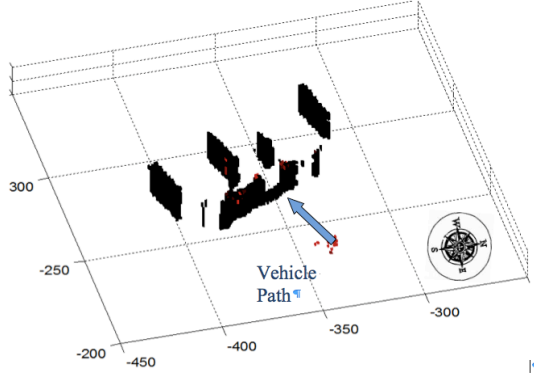
Figure 13. Occupancy grid developed with the vehicle on the southwest approach

6.0 SENSORY-BASED TRAJECTORIES

As apparent in the Figure 13, the free space available for the vehicle is small. It is defined by the cross section resolution obtained by the method described above. This free space can be expanded to the true distance between the pylons by navigating a trajectory over time that "points" the cross section of the FLS at the boundaries defined by the river surface and bottom and the nearest starboard and port bridge pylons. In other words, the environmental map is conservatively represented by limitations in the field of view of the cross section of the sonar. By ensonifying additional areas in front of the vehicle it improves map resolution and provides greater situational awareness for the vehicle.

A trajectory that increases the fidelity of the map through "pointing" the cross section of the forward looking sonar has two competing objectives; the ability to maintain a straight line path and the ability to fully ensonify a navigational hazard. Both of these objectives can be satisfied by a helix maneuver. Helical motion is obtained by using the cross-section beam model of the sonar and controlling the vehicle in such a way as to ensonify in a clockwise manner the starboard pylon, the water surface, the port pylon and the riverbed.

The control law that represents this helix motion can be parameterized in Cartesian coordinates by the following equations:

$$x(t) = \alpha t$$
$$y(t) = \beta \cos(t)$$
$$z(t) = \delta \sin(t)$$

where x, y, and z represents longitudinal, latitudinal and altitude positions for the AUV and α is a scalar for circular periodicity of the helix, β is the semi-major axis radius for the ellipse (as viewed in the y, z plane) and δ is semi-minor axis radius.

Define the bridge opening as ψ_o, as the difference between the vehicle headings when oriented toward the port and starboard pylon. Define the vertical opening as θ_o, as the difference between the water surface and riverbed.

$$\psi_O = \psi_{pp} - \psi_{sp}$$
$$\theta_O = \theta_{pp} - \theta_{sp}$$

The vertical and horizontal angles represented by ψ_o, θ_o increase as a function of speed and distance to the bridge. There are two interesting considerations in the development of the helical trajectory: First the commands to the rudder and dive plane are 90 degrees out of phase. Second, the amplitude of the commands are increasing this reflects the increasing aperture.

At some point the vehicle is unable to maintain the helical trajectory while maintaining a reasonable forward heading. This can be properly accounted for through the control parameters α, β, and δ. Figure 14 shows an example of initial results from testing helical trajectories in Monterey Bay, CA onboard the NPS REMUS AUV.

While more rigorous analysis is required, in general, the AUV must make a decision to move forward within approximately 20-30 meters of the obstacle.
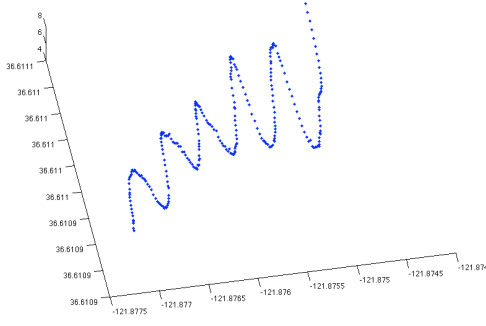
Figure 14. Helical Trajectory from the NPS REMUS in Monterey Bay, CA

6.0 FRENET-SERRET PATH FOLLOWING

An important consideration in the implementation of the helical trajectory is the ability of the controller to follow the calculated path over time. For the secondary controller this is accomplished through the kinematic path-following controller developed in [7]. Figure 16 depicts the coordinate frames used to develop this controller.
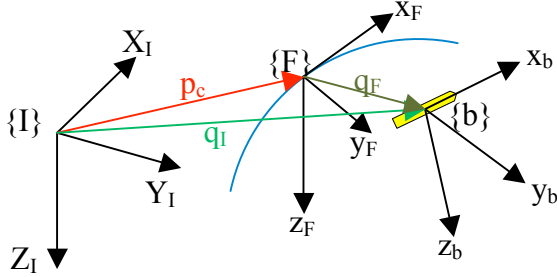
Figure 15. The inertial {I} frame, Serret-Frenet {F} error frame and the body-fixed reference frame describing the problem geometry.

Frame {I} is the inertial reference frame. Frame {F} is a Serret-Frenet frame attached to an arbitrary point on the path described by the vector p_c (red). Frame {b} is the body-fixed reference frame aligned with the AUV forward velocity vector. From this geometry, it is possible to establish a relationship between vector q_I, the inertial position of the AUV, and the vector q_F, its position of expressed in the Serret-Frenet frame attached to the spatial trajectory. This produces the simple kinematic model:

$$\dot{x}_I = U\cos\gamma\cos\psi$$
$$\dot{y}_I = U\cos\gamma\sin\psi$$
$$\dot{z}_I = -U\sin\gamma$$
$$\dot{\gamma} = q$$
$$\dot{\psi} = \frac{1}{\cos\gamma}r$$

where γ is the flight path angle above the horizontal plane and ψ is the heading angle.

Since the spatial trajectory is defined by the parametric equations above, it is a simple exercise to compute the tangent (T), normal (N), and binormal (B) unit vectors of frame {F}. In addition, the angular velocity of frame {F} with respect to the inertial frame {I}, resolved in {F} depends only upon the curvature, κ, and the torsion, ζ, of the Serret-Frenet frame. This angular velocity is proportional to the speed at which a virtual AUV traverses the curve, $\dot{l}$, where l is the path length of the curve. We can then combine the T, N, B unit vectors into the [TNB] rotation matrix from to represent rotation from the {F} to {I} frame. Now that we have the necessary equations to relate q_I, q_F, and p_c and how they evolve in time, we can create a state-space representation of the error kinematics—that is, the position and attitude (Euler angles) of the AUV body-fixed frame relative to the Serret-Frenet frame, which is the desired position and orientation for the vehicle to assume while traversing the helix. In this representation:

$$\dot{x}_F = -l(1-\kappa y_F) + U\cos\theta_e\cos\psi_e$$
$$\dot{y}_F = -l(\kappa x_F - \varsigma z_F) + U\cos\theta_e\sin\psi_e$$
$$\dot{z}_F = -l\varsigma y_F - U\sin\theta_e$$
$$\dot{\theta}_e = u_\theta$$
$$\dot{\psi}_e = u_\psi$$
$$\dot{l} = K_1 x_F + U\cos\theta_e\cos\psi_e$$

In the above kinematics, $\dot{l}$ controls the speed of the virtual AUV we wish to "follow," while u_θ and u_ψ are control inputs for pitch rate and turn rate, respectively, typically suitable for sending to a primary autopilot. Reference [7] contains a detailed development of the control input signals

u_θ and u_θ used to reduce the error kinematics to zero (i.e. drive the AUV onto the desired trajectory) and provides a proof of this controller's exponential stability. It should be stated that in its present form, the REMUS control protocol does not accept pitch rate commands. Therefore, in the preliminary experiments with this type of trajectory, the horizontal and vertical plane motions were de-coupled so that higher-level depth commands could be used to control the vertical motion. Experimental data may provide a means for controlling pitch rate by adjusting the profile of these depth commands. Figure 12 depicts the helical trajectory with the superimposed tangent, normal and binormal unit vectors of the body frame.
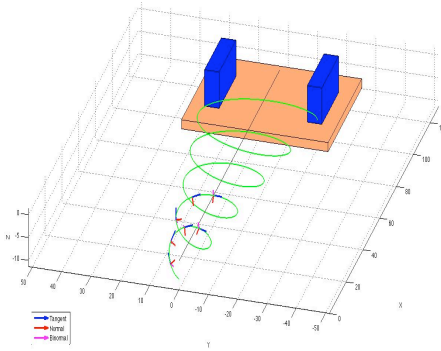
Figure 16. The AUV Helical Trajectory

6.0 CONCLUSIONS

In this paper, we demonstrated the ability to use complimentary sonar models to build a three dimensional probabilistic occupancy grid. This methodology was used to discover forward trajectories underneath a bridge that weren't otherwise available. A critical aspect to building the occupancy grid is a probability distribution for empty and occupied grid cells. A histogram approach was used for the generating these distributions. Results were demonstrated using a Charles River data set where the AUV navigated underneath the bridge avoiding the pylons. Finally a helical trajectory was introduced that permits the vehicle to fully take advantage of the cross section of the vertical and horizontal sonar while maintaining a forward path. Critical in developing non-traditional, non-linear AUV

paths are ensuring the vehicle can track the path, this is accomplished through the use of the kinematic path following controller utilizing the Frenet-Serret framework.

7.0 References

[1] Horner, D.P. , A.J. Healey, S.P. Kragelund, "AUV Experiments in Obstacle Avoidance", OCEANS, 2005. Proceedings of MTS/IEEE, 2005.

[2] Horner, D., and Yakimenko, O., "Recent Developments for an Obstacle Avoidance System for a Small AUV," Proceedings of the IFAC Conference on Control Applications in Marine Systems, Bol, Croatia, September 19-21, 2007.

[3] Yakimenko, O.A., Horner D.P., and Pratt, D.G., "AUV Rendezvous Trajectories Generation for Underwater Recovery," Proceedings of the 16th Mediterranean Conference on Control and Automation, Corse, France, June 25-27, 2008.

[4] Alberto Elfes, "Using Occupancy Grids for Mobile Robot Perception and Navigation," Computer, vol. 22, no. 6, pp. 46-57, June 1989.

[5] S. Thrun. et al Probabilistic Robotics. MIT Press 2005.

[6] F. Pedrotti, Pedrotti, L. Introduction to Optics, Prentice Hall 2007.

[7] Kaminer, I., Yakimenko, O.; Dobrokhodov, V.; Pascoal, A.; Hovakimyan, N.; Cao, C.; Young, A.; Patel, V. "Coordinated path following for time-critical missions of multiple UAVs via L1 adaptive output feedback controllers". AIAA Guidance, Navigation, and Control Conference 2007, v 1, p 915-948, 2007.